Critical optical-hysteresis regime and optical-bistability transformation

Jianning Li ⬤* and Dianzhen Cui ⬤

Center for Quantum Sciences and School of Physics, Northeast Normal University, Changchun 130024, China

In this paper, we study the optical-hysteresis regime in a driven-dissipative Bose-Hubbard dimer under a symmetric configuration and analyze the classical optical bistability with the Gross-Pitaevskii mean-field approach. We find that the critical point of the optical-hysteresis regime can be determined by the classical optical-bistability transformation predicted with a steady state equation, and the critical tunneling rate is given by analyzing the bistable threshold points. In addition, we apply the same approach to a single nonlinear microcavity coupled with an atom and the critical atom-cavity coupling strength of the optical-hysteresis regime is also obtained. Finally, in order to illustrate that the critical point could be determined by the classical optical-bistability transformation, we analyze the Liouvillian gap and find it opens at the critical point of the optical-hysteresis regime. This work clarifies the relation between optical hysteresis and classical optical bistability, which provides theoretical references for the modulation of optical hysteresis in experiment.

I. INTRODUCTION

In recent years, driven-dissipative systems have garnered a great deal of interest [1,2]. On the one hand, the physics could be calculated and predicted by the open quantum system theory (Lindbladian master equation) for both dynamics and steady states [3,4]. On the other hand, various experimental platforms and novel technologies have been developed and applied to driven-dissipative systems, which lead to interesting physical phenomena, such as unconventional magnetism [5], driven-dissipative superfluids [6], dissipative time crystals [7], etc. In particular, there is research emphasizing that a critical phenomenon could emerge in driven-dissipative systems [8,9], which is the so-called dissipative phase transition (DPT) [10–22]. In analogy to the quantum phase transition [23], the maximum real part of the nonzero Liouvillian superoperator eigenvalue, i.e., the Liouvillian gap, is discontinuous and approaches zero at the critical point [17–22], which leads to a long relaxation time to evolve to a steady state. With the advent of new technologies, the DPT has been probed via optical hysteresis in a nonlinear semiconductor microcavity experimentally [24]. Optical hysteresis is a nonadiabatic response while the parameter crosses the critical point of DPT [22] and is associated with the classical optical bistability predicted at the mean-field level.

As a current topic of intense research, the interesting properties of DPT inspire other experimental investigations [25–29] as well as theoretical studies in photonic resonators including the nonlinear Kerr model [30–32] and Bose-Hubbard model [33–35]. In quantum optics, the Bose-Hubbard dimer is a major platform for studying entanglement [36,37], spontaneous symmetry breaking [38], unconventional photon blockades [39,40], and bistable time

crystals [41]. In addition, there are studies exploring the self-trapping effect in Bose-Hubbard dimers [42–45]. To our knowledge, the critical tunneling rate of the self-trapping regime in a closed Bose-Hubbard dimer (or bosonic Josephson junction) could be solved strictly, which is dependent on the total photon numbers and the difference of initial photons between the two microcavities [46–48]. Unfortunately, it is difficult to obtain the critical tunneling rate for a driven-dissipative Bose-Hubbard dimer because the energy and particles are not conserved, so that the phase diagram of the steady state self-trapping regime (the photons are localized more in one of the microcavities corresponding to the symmetry-breaking state) is given in Ref. [45] numerically. Motivated by these studies of the critical tunneling rate for the self-trapping effect in a Bose-Hubbard dimer, we wonder how the tunneling rate affects the optical-hysteresis regime in a driven-dissipative scenario and whether can we obtain the critical tunneling rate? In addition, as emphasized in Ref. [34], the study of the nature of the critical tunneling rate is necessary for the optical-hysteresis regime. Therefore, how to pinpoint the exact location of the onset of the hysteresis regime should be considered. Here, we will give the answer and clarify the above issue.

In the present paper, we study the optical-hysteresis regime in a driven-dissipative Bose-Hubbard dimer, which consists of two coupled nonlinear microcavities with a dissipative setting and both of them are driven coherently. We first review the steady state self-trapping effect and give the expression for the steady state phase for two microcavities with the Gross-Pitaevskii mean-field approach. Then we investigate the hysteresis area versus the tunneling rate for different metastable residence times [27] and the results show that there is a critical point for the optical-hysteresis regime. We give the critical tunneling rate by analyzing the bistable threshold points under the symmetry-preserving steady state (the photon numbers are equal for two microcavities). The
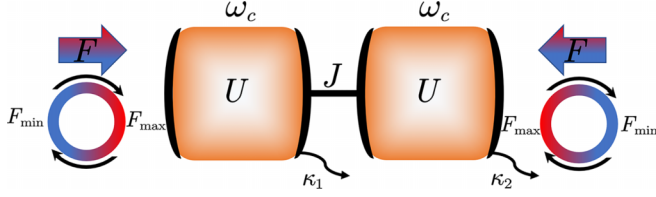
FIG. 1. A schematic of a driven-dissipative Bose-Hubbard dimer, where the two resonant microcavities (frequency ω_c) are coupled by tunneling (rate J) and filled with nonlinear media which induce effective photon-photon interactions (strength U). In addition, both microcavities are driven coherently with an external pumping laser whose amplitude F is adjustable. The dissipation rates of the two microcavities are κ_1 and κ_2, respectively.

semiclassical analysis shows the tunneling rate changes the resonance frequency of the microcavity so that the bistable region widens with an increasing tunneling rate beyond the critical point, which corresponds to two further branches leading to a large hysteresis area. Next, we explore the critical atom-cavity coupling strength of a single nonlinear microcavity coupled with an atom for the optical-hysteresis regime. The physics induced by the atom-cavity coupling are shown, weakening the Kerr nonlinearity, changing the resonant frequency and the dissipation rate of the microcavity, and the critical coupling strength of the optical-hysteresis regime is also obtained. Finally, in order to illustrate that the critical point could be determined by the classical optical-bistability transformation, we analyze the Liouvillian gap and find it opens at the critical point of the optical-hysteresis regime.

This paper is structured as follows: We introduce the physical model and theoretical approach, present some necessary expressions, and review the self-trapping effect in Sec. II. In Sec. III, we give the critical tunneling rate for the optical-hysteresis regime in a Bose-Hubbard dimer. Section IV is devoted to exploring the critical atom-cavity coupling strength of the optical-hysteresis regime and discuss the physical effects induced by the coupling. Section V shows the eigenvalues of the Liouvillian superoperator. Finally, we conclude and discuss the results in Sec. VI.

II. PHYSICAL MODEL AND THEORETICAL APPROACH

In this section, we first show the physical model and give the theoretical approach used in the following, including the Lindblad master equation and the Gross-Pitaevskii approach for a driven-dissipative Bose-Hubbard dimer, and the schematic of the dimer is shown in Fig. 1. Some expressions are given by reviewing the steady state self-trapping effect and we obtain the analytical solution for the steady state phase of the symmetry-preserving steady state under a symmetric configuration.

A. Physical model and master equation

The Bose-Hubbard dimer includes local Kerr nonlinearity in two microcavities which are coupled by tunneling. In addition, the microcavities are driven coherently in a dissipative

setting. The total Hamiltonian reads ($\hbar = 1$)

$$H = H_{\mathrm{BH}} + H_d(t),$$

$$H_{\mathrm{BH}} = \sum_{j=1,2}(\omega_c a_j^\dagger a_j + U a_j^\dagger a_j^\dagger a_j a_j) - J(a_1^\dagger a_2 + a_2^\dagger a_1),$$

$$H_d(t) = \sum_{j=1,2}(Fe^{-i\omega_d t} a_j^\dagger + F^* e^{i\omega_d t} a_j), \tag{1}$$

where $a_j^\dagger$ (a_j) are the creation (annihilation) operators for the two microcavities, respectively. ω_c is the resonant frequency of the microcavities and ω_d is the frequency of the drive. In the frame rotating with the driving frequency ω_d, which eliminates the time dependence and the relevant parameter, is the detuning $\Delta = \omega_c - \omega_d$. J denotes the tunneling rate and the terms with J represent the intercavity tunneling. U is the strength of the Kerr nonlinearity and F is the pumping amplitude of the coherent drive.

Within the Born-Markov approximation, the dissipative dynamics of the dimer reduced density matrix ρ is described by the quantum master equation in Lindbladian form,

$$\frac{\partial \rho}{\partial t} = -i[H, \rho] + \sum_{j=1,2} \kappa_j(2a_j \rho a_j^\dagger - a_j^\dagger a_j \rho - \rho a_j^\dagger a_j)$$

$$\equiv \mathcal{L}\rho, \tag{2}$$

where H is the Hamiltonian of the system and $\mathcal{L}$ is the Liouvillian superoperator. κ_1 and κ_2 denote the dissipation rate of the two microcavities, respectively. In the case $\kappa_1 = \kappa_2$, the master equation (2) has discrete $\mathbb{Z}_2$ symmetry described by the transformation $a_1 \leftrightarrow a_2$ [49], which means the steady state photon numbers are always equal for the two microcavities. One can find the unique and initial state-independent steady state ρ_{ss} by solving $\mathcal{L}\rho_{\mathrm{ss}} = 0$. The expectation value of an arbitrary operator O is calculated through $\langle O \rangle := \mathrm{Tr}[O\rho]$, where Tr denotes the trace over the system.

B. Self-trapping effect and steady state phase with the Gross-Pitaevskii approach

For a closed Bose-Hubbard dimer, we are concerned about the self-trapping effect of the dynamics due to the energy and the particles are conserved [46–48]. However, one is more concerned about the steady state self-trapping effect in such a driven-dissipative scenario [44,45]. In this section, we review the steady state self-trapping effect in a driven-dissipative Bose-Hubbard dimer and present some necessary expressions with the Gross-Pitaevskii mean-field approach, which will be used in the next section.

Ignoring quantum fluctuations, the mean-field amplitudes α_1 and α_2 for the operators a_1 and a_2 satisfy the following nonlinear equations:

$$i\frac{\partial}{\partial t}\alpha_1 = (\Delta + 2U|\alpha_1|^2 - i\kappa_1)\alpha_1 - J\alpha_2 + F,$$

$$i\frac{\partial}{\partial t}\alpha_2 = (\Delta + 2U|\alpha_2|^2 - i\kappa_2)\alpha_2 - J\alpha_1 + F. \tag{3}$$

We show the evolution of α_j in Figs. 2(a) and 2(b) for different initial conditions, where one shares the same steady state (symmetry-preserving state) and another shows the
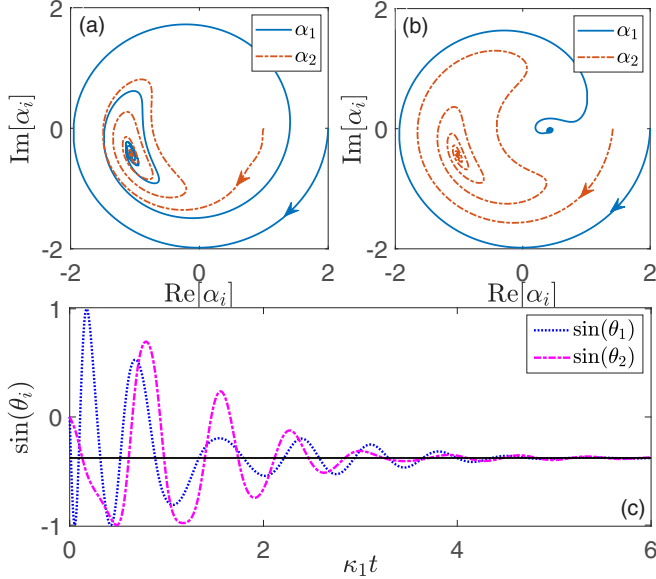
FIG. 2. (a) and (b) The trajectories describe the evolution of α_1 (blue solid line) and α_2 (orange dashed line) with the Gross-Pitaevskii mean-field approach. The initial conditions are $n_1 = 4$, $n_2 = 1$ for (a) and $n_1 = 4$, $n_2 = 2$ for (b). The arrows indicate how the fields evolve with an increase in time towards steady state. (c) The dotted and dashed-dotted lines show the evolution of the phase for α_1 and α_2, respectively, and the solid line is calculated by Eq. (6) with the symmetry-preserving steady state in (a). The system parameters chosen are $F = 3\kappa_1$, $J = 0.5\kappa_1$, $U = 5\kappa_1$, $\Delta = -10\kappa_1$, and $\kappa_1 = \kappa_2 = \kappa = 0.2 \times 2\pi$ GHz.

self-trapping steady state (symmetry-breaking state) [45]. Furthermore, we apply the transformation $\alpha_j = \tilde{\alpha}_j e^{i\theta_j}$, where θ_j are the phases for two microcavities and $n_j = |\alpha_j|^2$ are the photon numbers. By setting $\frac{\partial}{\partial t}\alpha_j = 0$, we obtain the following steady state equations,

$$|F|^2 = n_1\big[\kappa_1^2 + (2Un_1 + \Delta)^2\big] - 2\kappa_1 J\sqrt{n_1 n_2}\sin\delta\theta$$
$$- 2J\sqrt{n_1 n_2}(2Un_1 + \Delta)\cos\delta\theta + J^2 n_2,$$
$$|F|^2 = n_2\big[\kappa_2^2 + (2Un_2 + \Delta)^2\big] + 2\kappa_2 J\sqrt{n_1 n_2}\sin\delta\theta$$
$$- 2J\sqrt{n_1 n_2}(2Un_2 + \Delta)\cos\delta\theta + J^2 n_1, \quad (4)$$

where $\delta\theta = \theta_1 - \theta_2$ is the relative phase of two microcavities. Eliminate F in the equations and some algebra yields the following equation,

$$4\kappa J\sqrt{n_1 n_2}\sin\delta\theta = \Xi(n_1 - n_2), \quad (5)$$

where $\Xi = 4U^2(n_1^2 + n_2^2 + n_1 n_2) + 4U\Delta(n_1 + n_2) - 4UJ\sqrt{n_1 n_2}\cos\delta\theta + \kappa^2 + \Delta^2 - J^2$ and we have set $\kappa_1 = \kappa_2 = \kappa$. One can conclude if $n_1 = n_2$, $\delta\theta = 0$ and $n_1 \neq n_2$, $\delta\theta \neq 0$, which correspond to the symmetry-preserving and symmetry-breaking steady states shown in Figs. 2(a) and 2(b), respectively. Next, we give the expression of the symmetry-preserving steady state phase $\theta_1 = \theta_2 = \theta$, which is dependent on the system parameters in the case of a symmetric configuration,

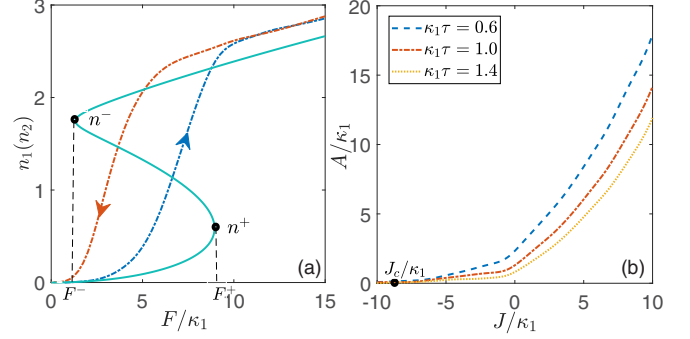$$\theta = \arcsin\left(-\frac{\kappa\sqrt{n}}{F}\right), \quad (6)$$

FIG. 3. (a) shows the photon numbers $n_j = \langle a_j^\dagger a_j \rangle$ as a function of the sweeping parameter F. The solid line denotes the solution with the Gross-Pitaevskii mean-field approach under the symmetry-preserving steady state using Eq. (8), and the dashed lines stand for the hysteresis loop calculated by the quantum master equation (2), where the arrows indicate the sweeping direction of F. n^- and n^+ are the photon numbers for the threshold points corresponding to different driving amplitudes F^- and F^+. (b) is plotted for the hysteresis area A as a function of the tunneling rate J for different metastable residence times τ. The black dot J_c corresponds to the hysteresis area $A = 0$. The parameter chosen is $N = 31$ and others are the same as in Fig. 2.

where $n = n_1 = n_2$ are the steady state photon numbers of the microcavities. As shown in Fig. 2(c), we give the evolution of θ_1 and θ_2 using dashed-dotted and dotted lines, respectively, and the solid line is calculated by Eq. (6) which accords well with the numerical results for the steady state.

III. OPTICAL-HYSTERESIS REGIME AND THE CRITICAL TUNNELING RATE

In this section, we study the optical-hysteresis regime by sweeping the adjustable driving amplitude with a triangular modulation [22] for both microcavities of the Bose-Hubbard dimer, which consists of an ascending order from F_0 to $F_0 + N\delta F$ and a descending order from $F_0 + N\delta F$ to F_0, and δF and N are the size and number of steps, where we keep $N\delta F$ a constant. We take the steady state by solving the master equation (2) at $F = F_0$ as an initial state, then sweep F in both ascending and descending order with a constant speed characterized by δF and the metastable residence time τ [27]. The results are shown by dashed-dotted lines in Fig. 3(a), where we plot the optical-hysteresis loop of the photon numbers $n_j = \langle a_j^\dagger a_j \rangle$. Next, in order to study the properties of optical hysteresis quantitatively, we define a hysteresis area enclosed by the hysteresis loop [20–22],

$$A = \int_{F_{\min}}^{F_{\max}} |n_\uparrow - n_\downarrow| dF, \quad (7)$$

where $\uparrow$ and $\downarrow$ denote the ascending and descending order of F, respectively. We plot A versus the tunneling rate for different τ in Fig. 3(b), where the results show that the strong tunneling rate corresponds to a large hysteresis area and the system is driven into the optical-hysteresis regime with an increase in J beyond a critical point. In addition, the critical point J_c can be determined by $A = 0$ which is marked with a black dot in Fig. 3(b). Next, we will give the critical tunneling
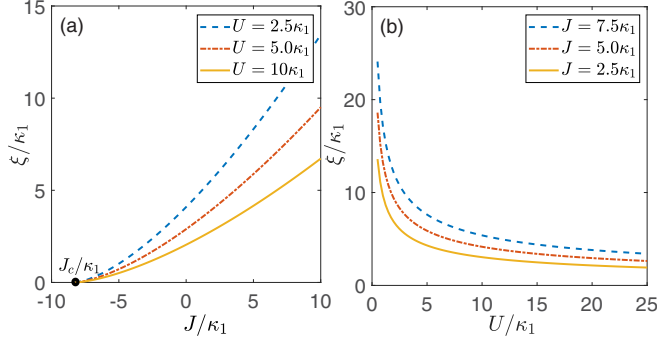
FIG. 4. (a) and (b) show the width of the bistable region ξ as a function of the tunneling rate J and Kerr nonlinearity strength U. As the black dot marked in (a), the critical tunneling rate J_c corresponding to $\xi = 0$ could be predicted by Eq. (10), which means a zero bistable region. The other system parameters are the same as in Fig. 2.

rate J_c by analyzing the bistable threshold points with the Gross-Pitaevskii mean-field approach based on Sec. II.

Considering the symmetric configuration of the two cavities, a discrete $\mathbb{Z}_2$ symmetry of master equation (2) is described by the transformation $a_1 \leftrightarrow a_2$ [49]. Therefore, it is reasonable to study the critical tunneling rate J_c under the symmetry-preserving steady state, i.e., $n_1 = n_2 = n$ and $\theta_1 = \theta_2 = \theta$. Thus, we obtain the simplified steady state equation,

$$|F|^2 = n[\kappa^2 + (2Un + \Delta - J)^2], \qquad (8)$$

where we have set $\kappa_1 = \kappa_2 = \kappa$. In particular, we notice that there is no limit for the sign of the tunneling rate J. A standard photonic dimer achieves a positive tunneling rate and negative tunneling devices can be implemented with coupled photonic crystal microcavities [50]. However, it brings different physical effects which decrease or increase the microcavity resonance frequency, respectively.

By analyzing the threshold points [marked by black dots in Fig. 3(a) with $n^{\pm}$] for optical bistability, we obtain the following photon numbers of the threshold points by setting $d|F|^2/dn = 0$ in Eq. (8),

$$n^{\pm} = \frac{-2(\Delta - J) \pm \sqrt{(\Delta - J)^2 - 3\kappa^2}}{6U}, \qquad (9)$$

the optical-instability region is between n^- and n^+. Furthermore, considering the photon numbers $n^{\pm}$ are always positive and real, it is clear that the optical bistability requires $(\Delta - J)U < 0$ and $(\Delta - J)^2 > 3\kappa^2$. Therefore, one can obtain the critical tunneling rate J_c for optical bistability (here, we only consider $U > 0$ for simplicity),

$$J_c = \Delta + \sqrt{3}\kappa. \qquad (10)$$

For $J > J_c$, the system is driven into the optical-bistability regime. In addition, we define ξ,

$$\xi = F^+ - F^-, \qquad (11)$$

to describe the width of the bistable region, where F^- and F^+ are marked in Fig. 3(a) corresponding to n^- and n^+, respectively. We plot ξ versus the tunneling rate J in Fig. 4(a)

and the results show the bistable region widens with increasing tunneling rate beyond the critical tunneling rate J_c. The wide bistable region corresponds to two further branches (the hysteresis loop) predicted by the master equation (2) which corresponds to the large hysteresis area in Fig. 3(b). Finally, in Fig. 4(b) we also show ξ decreases with increasing Kerr nonlinearity strength U. The fundamental physics is the Kerr nonlinearity increases the effective microcavity resonance frequency [51] which leads to a narrow bistable region.

IV. CRITICAL ATOM-CAVITY COUPLING STRENGTH FOR THE OPTICAL-HYSTERESIS REGIME

In the previous section, we have given the critical tunneling rate of the optical-hysteresis regime in a driven-dissipative Bose-Hubbard dimer. Here, we give the critical atom-cavity coupling strength for a single nonlinear microcavity coupled with an atom and discuss other physical effects induced by the coupling.

The time-independent Hamiltonian of the atom-cavity system reads ($\hbar = 1$)

$$H = -\Delta\left(a^{\dagger}a + \frac{1}{2}\sigma_z\right) + g(a\sigma_+ + \sigma_-a^{\dagger})$$
$$+ \frac{U}{2}a^{\dagger}a^{\dagger}aa + F(a + a^{\dagger}), \qquad (12)$$

where $a^{\dagger}$ and a are the creation and annihilation operators for the microcavity, respectively. σ_+ and σ_- are the raising and lowering operators for the atom where $\sigma_{\pm} = \frac{1}{2}(\sigma_x \pm i\sigma_y)$, σ_i, $i \in \{x, y, z\}$, are the Pauli operators. $\Delta = \omega_d - \omega_c$ is the drive-cavity detuning where ω_d and ω_c stand for the frequency of the drive and microcavity, respectively. g denotes the atom-cavity coupling strength, U is the strength of the Kerr nonlinearity, and F is the amplitude of the drive.

With the Gross-Pitaevskii mean-field approach, we obtain the following equations with Hamiltonian (12),

$$\dot{\alpha} = (i\Delta - iU|\alpha|^2 - \bar{\kappa})\alpha - ig\beta - iF, \qquad (13)$$

$$\dot{\beta} = -(\gamma_{\perp} - i\Delta)\beta + ig\alpha\chi, \qquad (14)$$

$$\dot{\chi} = 2ig(\alpha^*\beta - \alpha\beta^*) - \gamma_{\parallel}(\chi + 1), \qquad (15)$$

where $\alpha = \langle a \rangle$, $\beta = \langle \sigma_- \rangle$, and $\chi = \langle \sigma_z \rangle$. $\bar{\kappa}$ is the dissipation rate of the microcavity, and $\gamma_{\perp}$ and $\gamma_{\parallel}$ denote the transverse and longitudinal relaxation rates of the atom, respectively [52]. Some algebra yields the steady state solutions of α and χ,

$$\alpha = \frac{iF}{i\Delta - \bar{\kappa} - iU|\alpha|^2 + \frac{g^2\chi}{\gamma_{\perp} - i\Delta}}, \qquad (16)$$

$$\chi = \frac{-1}{1 + \frac{4g^2|\alpha|^2}{\gamma_{\perp}\gamma_{\parallel}\left(1 + \frac{\Delta^2}{\gamma_{\perp}^2}\right)}}. \qquad (17)$$

Here, we consider the linear relation $\gamma_{\perp} = m\gamma_{\parallel}$ where m is a constant. In this case, the results reduce to

$$\alpha = \frac{iF}{i\Delta - \bar{\kappa} - iU|\alpha|^2 - \frac{g^2(\gamma_{\perp} + i\Delta)}{\gamma_{\perp}^2 + \Delta^2 + 4mg^2|\alpha|^2}}. \qquad (18)$$
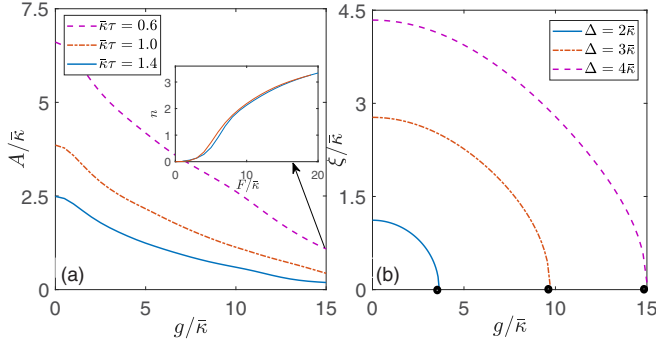
FIG. 5. (a) shows the hysteresis area A as a function of the atom-cavity coupling strength g for different τ. The inset is the nearly enclosed hysteresis loop for the critical point g_c. (b) shows ξ as a function of g for different detuning Δ. The critical point g_c marked by black dots for $\xi = 0$ are calculated by Eq. (22). The system parameters are $\gamma_\perp = 0.01\bar{\kappa}$ and $m = 0.02\bar{\kappa}$.

In the weak-coupling regime defined by [9]

$$4mg^2|\alpha|^2 \ll \Delta^2, \tag{19}$$

and considering $\gamma_\perp$ is very small compared to the detuning Δ [52], we obtain

$$\alpha = \frac{iF}{-i\tilde{U}|\alpha|^2 + i\tilde{\Delta} - \tilde{\kappa}}, \tag{20}$$

where

$$\tilde{U} = U - \frac{4mg^4}{\Delta^3}, \quad \tilde{\Delta} = \Delta + \frac{g^2\gamma_\perp^2}{\Delta^3} - \frac{g^2}{\Delta},$$

$$\tilde{\kappa} = \bar{\kappa} + \frac{g^2\gamma_\perp}{\Delta^2} - \frac{g^2\gamma_\perp^3}{\Delta^4}, \tag{21}$$

are the effective Kerr nonlinear strength, detuning, and dissipation rate, respectively, which result from the interaction between the atom and the microcavity. The term with $-\frac{4mg^4}{\Delta^3}$ weakens the Kerr nonlinearity [53]. $\frac{g^2\gamma_\perp^2}{\Delta^3} - \frac{g^2}{\Delta}$ and $\frac{g^2\gamma_\perp}{\Delta^2} - \frac{g^2\gamma_\perp^3}{\Delta^4}$ change the resonant frequency and the dissipation rate of the microcavity. We show the hysteresis area versus the coupling strength in Fig. 5(a). In principle, the coupling weakens the Kerr nonlinearity which should lead to a large hysteresis area with increasing g. However, it is not the case because the coupling also decreases the resonance frequency of the microcavity which makes it far away from the optical-hysteresis regime, and the latter generates the main effect. Furthermore, we give the critical atom-cavity coupling strength g_c,

$$g_c = \sqrt{\frac{\sqrt{3}\bar{\kappa}\Delta^4 - \Delta^5}{\gamma_\perp^2\Delta - \Delta^3 - \sqrt{3}\gamma_\perp\Delta^2 + \sqrt{3}\gamma_\perp^3}}. \tag{22}$$

For $g < g_c$, the microcavity is driven into the optical-bistability regime. As the discussion in Ref. [52], $\gamma_\perp \ll \Delta$, and we can obtain the following expression of g_c,

$$g_c = \sqrt{\Delta^2 - \sqrt{3}\bar{\kappa}\Delta}. \tag{23}$$

Finally, we numerically calculate the width of the bistable region ξ versus the atom-cavity coupling strength and show
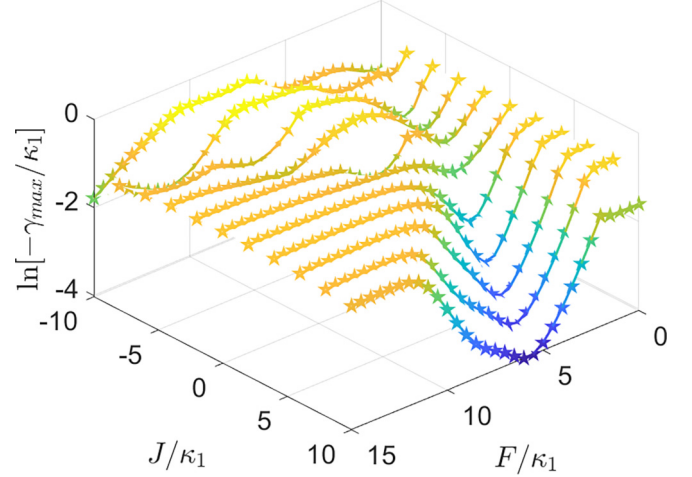

FIG. 6. The maximum real part of the non-zero Liouvillian eigenvalue $\ln[-\gamma_{\max}]$ vs F and J in a driven-dissipative Bose-Hubbard dimer. The result shows that the Liouvillian gap is opened with decreasing J. Meanwhile, the width of the bistable region ξ is narrow as shown in Fig. 4(a) and the hysteresis area also decreases in Fig. 3(b). The parameters chosen are the same as in Fig. 2.

the results in Fig. 5(b). As expected, it decreases with increasing g, and the critical coupling strength for $\xi = 0$ could be predicted by Eq. (22), which are marked by black dots corresponding to the closed hysteresis loop as shown in the inset in Fig. 5(a).

V. ANALYSIS OF THE LIOUVILLIAN GAP

In the previous sections, we have studied the optical-hysteresis regime and given the critical points in a driven-dissipative Bose-Hubbard dimer and the single nonlinear microcavity coupled with an atom. In order to illustrate that the critical points of the optical-hysteresis regime could be determined by analyzing the bistable threshold points of a classical optical-bistability transformation, we analyze the behavior of the Liouvillian gap near the critical point in the following.

The eigenvalues of the Liouvillian superoperator are complex, $\lambda = \gamma + i\omega$, because of its non-Hermiticity. Also, the real parts of the eigenvalues are nonpositive, namely, $\gamma \leqslant 0$, which ensure the existence of a steady state. The maximum real part of the nonzero eigenvalue (the Liouvillian gap) determines the relaxation time to the steady state [3,4]. More specifically, a narrower gap corresponds to a longer relaxation time. We show the Liouvillian gap in Figs. 6 and 7 for the Bose-Hubbard dimer and atom-cavity system, respectively. In Fig. 6, the different curves correspond to different tunneling rates J, and the dip vanishes with decreasing J until the critical point predicted by the classical bistability transformation [see the critical point in Fig. 4(a) calculated by Eq. (10)], which means the Liouvillian gap is opened, leading to the zero hysteresis area [see $A = 0$ in Fig. 3(b)]. Similarly, as the results shown in Fig. 7 for an atom-cavity system, we analyze the corresponding eigenvalue and the dip vanishes with increasing g until the critical atom-cavity coupling strength given by
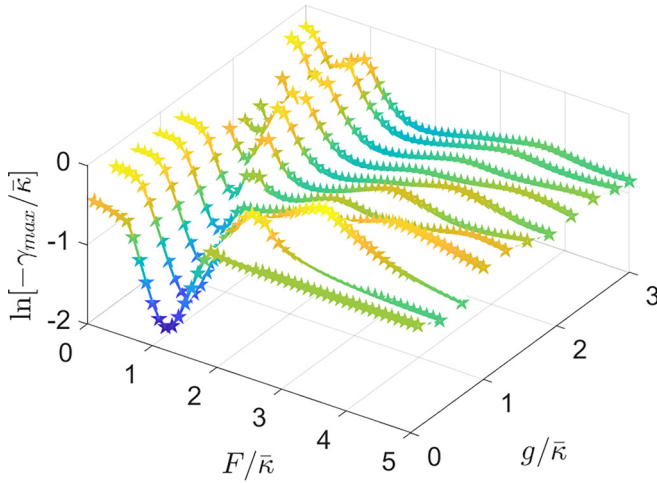
FIG. 7. The maximum real part of the nonzero Liouvillian eigenvalue $\ln[-\gamma_{max}]$ vs F and g in an atom-cavity system. The Liouvillian gap is opened with increasing g. The parameters chosen are the same as in Fig. 5.

Eq. (22) and the hysteresis area is closed to zero as shown in Fig. 5(a). Correspondingly, the bistable region becomes narrow with increasing g. Therefore, the critical point of the optical-hysteresis regime could be predicted by analyzing the classical optical-bistability transformation.

VI. CONCLUSION

In this paper, we have studied the optical-hysteresis regime in a driven-dissipative Bose-Hubbard dimer and the critical tunneling rate has been given with the Gross-Pitaevskii mean-field approach by analyzing the bistable threshold points. We have given the steady state phase for symmetric microcavities under a symmetry-preserving steady state. In addition, we have studied the critical atom-cavity coupling strength of a single nonlinear microcavity coupled with an atom for the optical-hysteresis regime. The critical atom-cavity coupling has been obtained and we have discussed the physical effects induced by the coupling, which weakens the Kerr nonlinearity, and changes the resonance frequency and the dissipation rate of the microcavity. Finally, we have analyzed the Liouvillian gap and the results show that it opens at the critical point of the optical-hysteresis regime, which means that the critical point can be determined by the classical optical-bistability transformation exactly. This work have clarified the relation between optical hysteresis and classical optical bistability, which provides theoretical references for the modulation of optical hysteresis in experiment.

[1] I. Carusotto and C. Ciuti, Quantum fluids of light, Rev. Mod. Phys. **85**, 299 (2013).

[2] S. Schmidt and J. Koch, Circuit QED lattices: Towards quantum simulation with superconducting circuits, Ann. Phys. **525**, 395 (2013).

[3] H. P. Breuer and F. Petruccione, *The Theory of Open Quantum Systems* (Oxford University Press, Oxford, U.K., 2007).

[4] Á. Rivas and S. F. Huelga, *Open Quantum Systems: An Introduction*, Springer Briefs in Physics (Springer, Berlin, 2011).

[5] T. E. Lee, S. Gopalakrishnan, and M. D. Lukin, Unconventional Magnetism via Optical Pumping of Interacting Spin Systems, Phys. Rev. Lett. **110**, 257204 (2013).

[6] R. Labouvie, B. Santra, S. Heun, H. Ott, and M. D. Lukin, Bistability in a Driven-Dissipative Superfluid, Phys. Rev. Lett. **116**, 235302 (2016).

[7] H. Keßler, P. Kongkhambut, C. Georges, L. Mathey, J. G. Cosme, and A. Hemmerich, Observation of a Dissipative Time Crystal, Phys. Rev. Lett. **127**, 043602 (2021).

[8] E. M. Kessler, G. Giedke, A. Imamoglu, S. F. Yelin, M. D. Lukin, and J. I. Cirac, Dissipative phase transition in a central spin system, Phys. Rev. A **86**, 012116 (2012).

[9] H. J. Carmichael, Breakdown of Photon Blockade: A Dissipative Quantum Phase Transition in Zero Dimensions, Phys. Rev. X **5**, 031028 (2015).

[10] H. J. Carmichael, Analytical and numerical results for the steady state in cooperative resonance fluorescence, J. Phys. B **13**, 3551 (1980).

[11] P. Werner, K. Völker, M. Troyer, and S. Chakravarty, Phase Diagram and Critical Exponents of a Dissipative Ising Spin Chain in a Transverse Magnetic Field, Phys. Rev. Lett. **94**, 047201 (2005).

[12] L. Capriotti, A. Cuccoli, A. Fubini, V. Tognetti, and R. Vaia, Dissipation-Driven Phase Transition in Two-Dimensional Josephson Arrays, Phys. Rev. Lett. **94**, 157001 (2005).

[13] M. J. Bhaseen, J. Mayoh, B. D. Simons, and J. Keeling, Dynamics of nonequilibrium Dicke models, Phys. Rev. A **85**, 013817 (2012).

[14] S. Diehl, A. Tomadin, A. Micheli, R. Fazio, and P. Zoller, Dynamical Phase Transitions and Instabilities in Open Atomic Many-Body Systems, Phys. Rev. Lett. **105**, 015702 (2010).

[15] S. S. Sahoo, S. S. Nayak, S. R. Mishra, and A. K. Mohapatra, Dissipative phase transition in a mirrorless optical parametric oscillator, Phys. Rev. A **102**, 053724 (2020).

[16] J. Gosner, B. Kubala, and J. Ankerhold, Relaxation dynamics and dissipative phase transition in quantum oscillators with period tripling, Phys. Rev. B **101**, 054501 (2020).

[17] M.-J. Hwang, P. Rabl, and M. B. Plenio, Dissipative phase transition in the open quantum Rabi model, Phys. Rev. A **97**, 013825 (2018).

[18] W. Casteels, R. Fazio, and C. Ciuti, Critical dynamical properties of a first-order dissipative phase transition, Phys. Rev. A **95**, 012128 (2017).

[19] F. Minganti, A. Biella, N. Bartolo, and C. Ciuti, Spectral theory of Liouvillians for dissipative phase transitions, Phys. Rev. A **98**, 042118 (2018).

[20] D. O. Krimer and M. Pletyukhov, Few-Mode Geometric Description of a Driven-Dissipative Phase Transition in an Open Quantum System, Phys. Rev. Lett. **123**, 110604 (2019).

[21] J. Li, H. Z. Shen, W. Wang, and X. Yi, Atom-modulated dynamic optical hysteresis in driven-dissipative systems, Phys. Rev. A **104**, 013709 (2021).

[22] W. Casteels, F. Storme, A. Le Boité, and C. Ciuti, Power laws in the dynamic hysteresis of quantum nonlinear photonic resonators, Phys. Rev. A **93**, 033824 (2016).

[23] S. Sachdev, *Quantum Phase Transitions* (Cambridge University Press, Cambridge, U.K., 2001).

[24] S. R. K. Rodriguez, W. Casteels, F. Storme, N. Carlon Zambon, I. Sagnes, L. Le Gratiet, E. Galopin, A. Lemaître, A. Amo, C. Ciuti, and J. Bloch, Probing a Dissipative Phase Transition via Dynamical Optical Hysteresis, Phys. Rev. Lett. **118**, 247402 (2017).

[25] M. Fitzpatrick, N. M. Sundaresan, A. C. Y. Li, J. Koch, and A. A. Houck, Observation of a Dissipative Phase Transition in a One-Dimensional Circuit QED Lattice, Phys. Rev. X **7**, 011016 (2017).

[26] T. Fink, A. Schade, S. Höfling, C. Schneider, and A. Imamoglu, Signatures of a dissipative phase transition in photon correlation measurements, Nat. Phys. **14**, 365 (2018).

[27] Z. Geng, K. J. H. Peters, A. A. P. Trichet, K. Malmir, R. Kolkowski, J. M. Smith, and S. R. K. Rodriguez, Universal Scaling in the Dynamic Hysteresis, and Non-Markovian Dynamics, of a Tunable Optical Cavity and Non-Markovian Dynamics, of a Tunable Optical Cavity, Phys. Rev. Lett. **124**, 153603 (2020).

[28] Z. Li, F. Claude, T. Boulier, E. Giacobino, Q. Glorieux, A. Bramati, and C. Ciuti, Dissipative Phase Transition with Driving-Controlled Spatial Dimension and Diffusive Boundary Conditions, Phys. Rev. Lett. **128**, 093601 (2022).

[29] J. Benary, C. Baals, E. Bernhart, J. Jiang, M. Röhrle, and H. Ott, Experimental observation of a dissipative phase transition in a multi-mode many-body quantum system, New J. Phys. **24**, 103034 (2022).

[30] T. L. Heugel, M. Biondi, O. Zilberberg, and R. Chitra, Quantum Transducer Using a Parametric Driven-Dissipative Phase Transition, Phys. Rev. Lett. **123**, 173601 (2019).

[31] B. O. Goes and G. T. Landi, Entropy production dynamics in quench protocols of a driven-dissipative critical system, Phys. Rev. A **102**, 052202 (2020).

[32] B. O. Goes, C. E. Fiore, and G. T. Landi, Quantum features of entropy production in driven-dissipative transitions, Phys. Rev. Res. **2**, 013136 (2020).

[33] F. Vicentini, F. Minganti, R. Rota, G. Orso, and C. Ciuti, Critical slowing down in driven-dissipative Bose-Hubbard lattices, Phys. Rev. A **97**, 013853 (2018).

[34] D. Huybrechts and M. Wouters, Dynamical hysteresis properties of the driven-dissipative Bose-Hubbard model with a Gutzwiller Monte Carlo approach, Phys. Rev. A **102**, 053706 (2020).

[35] A. Le Boité, G. Orso, and C. Ciuti, Bose-Hubbard model: Relation between driven-dissipative steady states and equilibrium quantum phases, Phys. Rev. A **90**, 063821 (2014).

[36] W. Casteels and M. Wouters, Optically bistable driven-dissipative Bose-Hubbard dimer: Gutzwiller approaches and entanglement, Phys. Rev. A **95**, 043833 (2017).

[37] W. Casteels and C. Ciuti, Quantum entanglement in the spatial-symmetry-breaking phase transition of a driven-dissipative Bose-Hubbard dimer, Phys. Rev. A **95**, 013812 (2017).

[38] V. Savona, Spontaneous symmetry breaking in a quadratically driven nonlinear photonic lattice, Phys. Rev. A **96**, 033826 (2017).

[39] T. C. H. Liew and V. Savona, Single Photons from Coupled Quantum Modes, Phys. Rev. Lett. **104**, 183601 (2010).

[40] M. Bamba, A. Imamoğlu, I. Carusotto, and C. Ciuti, Origin of strong photon antibunching in weakly nonlinear photonic molecules, Phys. Rev. A **83**, 021802(R) (2011).

[41] C. Lledó, Th. K. Mavrogordatos, and M. H. Szymańska, Driven Bose-Hubbard dimer under nonlocal dissipation: A bistable time crystal, Phys. Rev. B **100**, 054303 (2019).

[42] T. Pudlik, H. Hennig, D. Witthaut, and D. K. Campbell, Tunneling in the self-trapped regime of a two-well Bose-Einstein condensate, Phys. Rev. A **90**, 053610 (2014).

[43] A. Dey and A. Vardi, Self-trapping of excitations: Two-dimensional quasiparticle solitons in an extended Bose-Hubbard dimer array, Phys. Rev. A **95**, 033630 (2017).

[44] M. Seclì, M. Capone, and M. Schirò, Signatures of self-trapping in the driven-dissipative Bose-Hubbard dimer, New J. Phys. **23**, 063056 (2021).

[45] B. Cao, K. W. Mahmud, and M. Hafezi, Two coupled nonlinear cavities in a driven-dissipative environment, Phys. Rev. A **94**, 063805 (2016).

[46] A. Smerzi, S. Fantoni, S. Giovanazzi, and S. R. Shenoy, Quantum Coherent Atomic Tunneling between Two Trapped Bose-Einstein Condensates, Phys. Rev. Lett. **79**, 4950 (1997).

[47] D. Sarchi, I. Carusotto, M. Wouters, and V. Savona, Coherent dynamics and parametric instabilities of microcavity polaritons in double-well systems, Phys. Rev. B **77**, 125324 (2008).

[48] M. Albiez, R. Gati, J. Fölling, S. Hunsmann, M. Cristiani, and M. K. Oberthaler, Direct Observation of Tunneling and Nonlinear Self-Trapping in a Single Bosonic Josephson Junction, Phys. Rev. Lett. **95**, 010402 (2005).

[49] A. Giraldo, B. Krauskopf, N. G. R. Broderick, J. A. Levenson, and A. M. Yacomotti, The driven-dissipative Bose-Hubbard dimer: phase diagram and chaos, New J. Phys. **22**, 043009 (2020).

[50] S. Haddadi, P. Hamel, G. Beaudoin, I. Sagnes, C. Sauvan, P. Lalanne, J. A. Levenson, and A. M. Yacomotti, Photonic molecules: tailoring the coupling strength and sign, Opt. Express **22**, 12359 (2014).

[51] P. D. Drummond and D. F. Walls, Quantum theory of optical bistability. I: Nonlinear polarisability model, J. Phys. A: Math. Gen. **13**, 725 (1980).

[52] D. O. Krimer, M. Zens, and S. Rotter, Critical phenomena and nonlinear dynamics in a spin ensemble strongly coupled to a cavity. I. Semiclassical approach, Phys. Rev. A **100**, 013855 (2019).

[53] The optical bistability requests $U\Delta > 0$ according to the definition of Δ in Ref. [21], so that the term with $-\frac{4mg^4}{\Delta^3}$ weakens the Kerr nonlinearity.